Giant magnetostrictive nanostructured films with auto induced spin reorientation transition

Yannick Dusch, Nicolas Tiercelin, A. Klimov, V. Rudenko, Y. Ignatov, S. Hage-Ali, Philippe Pernod, Vladimir Preobrazhensky

Giant magnetostrictive nanostructured films with auto induced spin reorientation transition

Yannick Dusch,[a] Nicolas Tiercelin, Alexey Klimov, Vasyl Rudenko, Yury Ignatov, Sami Hage-Ali, Philippe Pernod, and Vladimir Preobrazhensky
International Associated Laboratory LEMAC:
IEMN, UMR CNRS 8520, PRES Lille Nord de France, ECLille, 59651 Villeneuve d'Ascq, France
Wave Research Center, GPI RAS, 38 Vavilov str., Moscow, 119991, Russia
Moscow Institute of Radiotechniques, Electrical engineering and Automation, Moscow, Russia
V. A. Kotel'nikov Institute of Radioengineering and Electronics RAS, 125009 Moscow, Russia

(Dated: 25 October 2010)

In various micro and nanosystems applications comprising magnetic films, the polarizing field still needs to be integrated. We hereby present a solution for self biasing of magnetic films using micropatterned permanent magnets. Micromagnetic simulations were used as a designing and optimization tool to create a biasing structure. Samples were elaborated with varying geometric parameters using classical silicon microfabrication techniques. Nanostructured TbCo/FeCo magnetostrictive thin films were sputtered over coercive FePt filled trenches etched in silicon. Magnetic and magnetoelastic characterizations confirmed numerical simulations. In particular, non-linear actuation of a self-biased magnetostrictive cantilever has been obtained at zero external polarizing field.

I. INTRODUCTION

It was shown that nanostructured giant magnetostrictive films[1–4] under Spin Reorientation Transition (SRT) can be made highly sensitive to magnetic excitations and exhibit strong non-linear behavior[5–7]. This feature of SRT conditions opens route toward, for example, original magnetoelectric microsensors, microactuators or RF devices[8–11]. In particular, magnetoelectric effect is dramatically enhanced near SRT in composite magnetostrictive/piezoelectric layered structures[12–14]. Such critical state can be obtained when the bias field H_{Bias} directed along the hard axis of magnetization (HA) reaches the anisotropy field H_a of the layer (field-induced SRT).

Polarization of magnetic layers in Micro and Nano-Electro-Mechanical-Systems (MEMS and NEMS) can be obtained by several means, depending on the requirements of the application. Macroscopic magnets can be used in research or industrial environments but prevent any size reduction of the systems. Spintronic devices or NEMS can benefit from thin exchange coupled layers. Nevertheless, due to the short length of the interactions, such nanostructures are hard to implement for thick active layers in the $100nm - 1\mu m$ range. The use of permanent magnet-induced boundary fields has also been investigated using SmCo[15] or CoPt[16] and was proved efficient for biasing magnetoresistive layers up to $200nm$ and several hundred oersteds. In any case, the typical length of the system along the biasing direction did not exceed a few hundred microns.

We hereby propose the use of micropatterned $L1_0$-FePt sputtered films to polarize magnetic thin films with larger in-plane dimensions.

- Part II will explain the benefits of SRT.
- Part III will deal with the biasing structure design and simulations.
- Technological process and results are given in IV and discussed in V

II. PROPERTIES OF NANOSTRUCTURED GIANT MAGNETOSTRICTIVE THIN FILMS UNDER SRT

Geometry of the basic unimorph actuator under consideration is presented in fig.1. It consists in a cantilever with magnetostrictive multilayer deposited on the surface. Orientations of the bias H_s and alternating h magnetic fields and magnetization M relatively to the easy axis (EA) of the multilayer are also shown in the figure. The magnetic free energy of the system can simply be written as the sum of the Zeeman energy and the anisotropy energy restricted at its first term:

$$F = -M(H_s cos(\varphi) + h sin(\varphi) + \frac{1}{2} H_a sin^2(\varphi))) \quad (1)$$

where H_a is the in-plane anisotropy field. This energy can then be used to understand the behavior of the magnetization angle φ. When the bias field is perpendicular to the EA and strong enough ($H_s > H_a$) magnetization is parallel to H_s and this orientation is stable. Application of an alternating field with an amplitude of a few

[a] Electronic mail: yannick.dusch@centraliens-lille.org

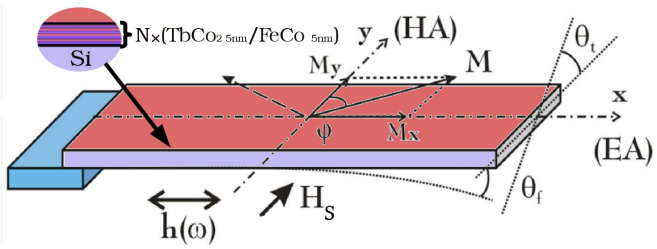

FIG. 1. Unimorph geometry : clamped silicon cantilever coated by a nanostructured magnetostrictive film.

Oersteds perpendicularly to H_s leads to a linear oscillation of the magnetization with a small angular amplitude (Fig.2a). The torsion elastic vibrations are linearly excited in such conditions. In the point of SRT ($H_s = H_a$), the magnetic subsystem becomes unstable. The amplitude of magnetic oscillation increases (Fig.2b) and nonlinearity manifests itself. When $H_s < H_a$ equilibrium orientation of magnetization turns towards the anisotropy axis (angular phase) and linear oscillation near the new equilibrium position takes place when amplitude h is not too high (Fig.2c). Rotation of magnetization leads also to appearance of longitudinal components of magnetostrictive stress and as a result to excitation of flexural deformations of cantilever. The dependence of magnetization angle on instantaneous value of alternating field is shown in Fig.2d. As expected for the SRT, this kind of behaviour is consistent with the second order phase transitions theory described by Landau[17]. Near the SRT, an increase of amplitude of the alternating field leads to a dramatic change of the thermodynamic potential (see Fig.3b) and the magnetic oscillation presents a switching character of its orientation between positions defined by the amplitude h: This switch is accompanied by a related switch of the magnetostrictive stress (as also observed in[18]). The spectrum of magnetic stress near SRT contains a great number of harmonics with high amplitudes. Each one can be used for resonance excitation of elastic modes. These properties are to be used in original MEMS or electronic devices. The following part describes the found solution for an integrated bias field structure.

III. NUMERICAL SIMULATIONS

As shown on fig.4, the biasing structure consists in parallel FePt trenches etched in a silicon substrate on top of which a Ta spacer and a (TbCo($5nm$)/FeCo($5nm$))*n multilayer are deposited. The multilayer exhibits uniaxial magnetic anisotropy. The easy axis of magnetization (EA) is obtained in the multilayer thanks to sputtering under magnetic field. Magnetostatic simulations of the flux density show that alternate polarized areas are created in the active layer, thanks to the coupled or isolated flux closure (fig.5). This leads to a striped magnetic structure in the active layer (part 1 and part 2,

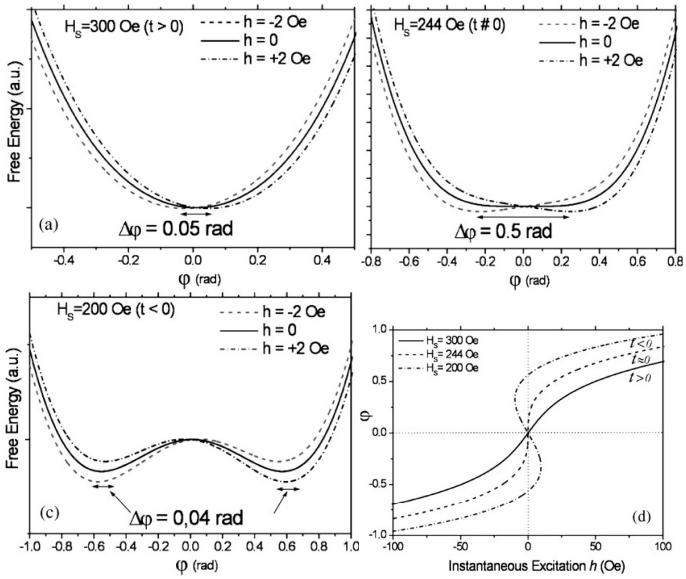

FIG. 2. Free energy of the system as a function of the magnetization angle φ, for several values of the excitation field $h(t)$ and for tree different positions of H_s: (a) $H_s > H_a$, (b) $H_s = H_a$, (c) $H_s < H_a$. In this simulation[5], $H_a = 244Oe$

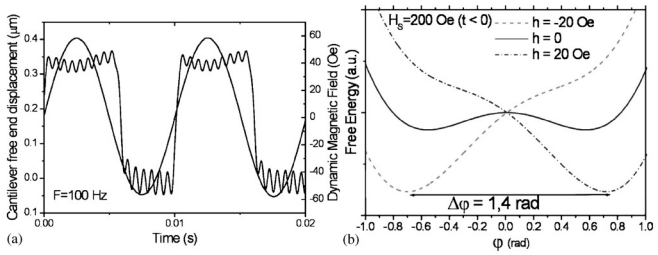

FIG. 3. Bistable behavior of the system[5]: (a) torsion response of the unimorph to the oscillating driving field. (b) Large displacement of the minimum of the free energy when this driving field is applied.

as shown in fig.4). The shape of the global hysteresis curve of the active layer along HA can be evaluated by superposing the two shifted curves of the stripes, as illustrated in fig.6a. Both parts exhibit a Stoner-Wohlfarth like rotation of magnetization.

Using the open source micromagnetic simulation software Magpar[21], we investigated the effects of several biasing structures on a magnetic thin film with in-plane uniaxial anisotropy. It appeared that the structure presented above offered a good tradeoff between the obtained polarization along HA and technological simplicity. Fig.6b presents a typical result of the numerical simulations, clearly showing the stripped pattern of magnetization on top of the active layer. Magpar has then been used to carry out numerous simulations with varying geometric parameters (FePt/silicon width ratio, trenches width, FePt thickness, Ta gap thickness) to optimize the strength and the homogeneity of the bias field.

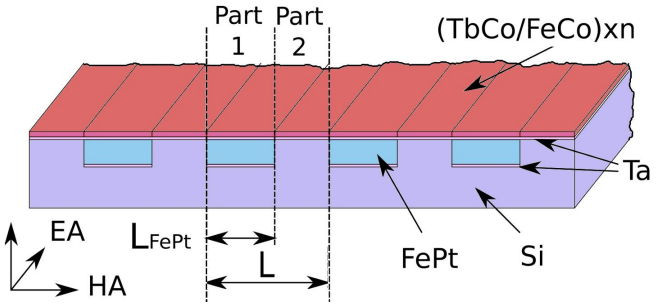

FIG. 4. Schematic view of the biasing structure[19].

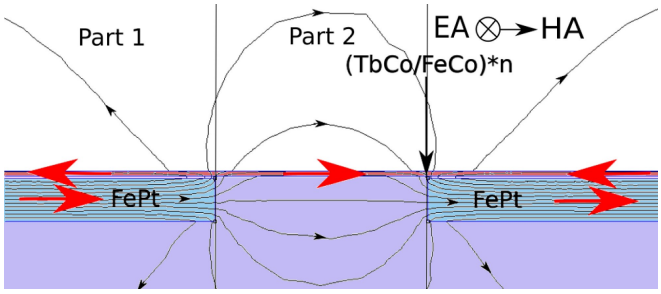

FIG. 5. Simulated flux lines (Femm[20]). Arrows indicate the main direction of magnetization[19].

IV. TECHNOLOGICAL PROCESS AND REALIZATION

Filled trenches of hard magnetic material have already been realized with SmCo and NdFeB, but the process involved a critical phase of Chemical-Mechanical-Planarization (CMP)[22]. We present here a simpler process for FePt, based on lift-off.

Prototypes were realized on Si wafers by usual microfabrication techniques in a cleanroom environment. Silicon is first etched through an aluminum mask by means of Deep Reactive Ion Etching (DRIE) down to $2\mu m$. A $100nm$ Ta adhesive layer as well as a thick ($2\mu m$) FePt layer are then deposited by RF Sputtering. Lift-off is used to remove the excess material. FePt is obtained by

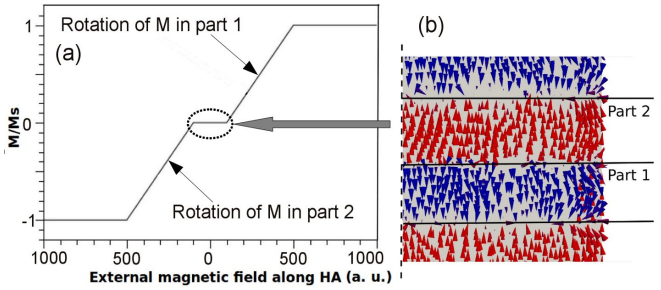

FIG. 6. (a): Schematic illustration of the magnetization curve of the active layer when the polarizing field is superior to the anisotropy field. (b): Top view of the simulated active layer with $H_{ext} = 0Oe$, $L_{FePt} = 25\mu m$ and $L = 50\mu m$. Arrows indicate magnetization.

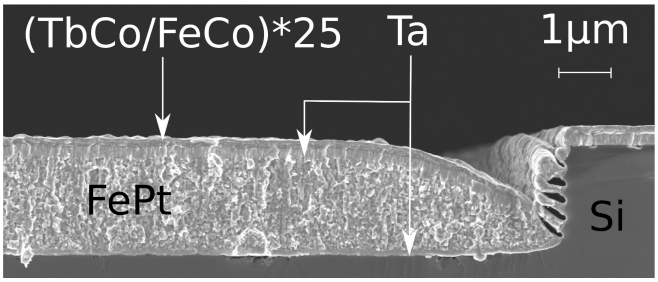

FIG. 7. SEM view of the processed microstructure[19].

the RF sputtering of a composite target under Ar flow at $5.10^{-3}mbar$. Sputtering is decomposed into $15min$ runs followed by a rest period of $4min$ to prevent detrimental effects of temperature, such as internal stress. A $100nm$ Ta non-magnetic spacer (also used to prevent oxydation of FePt during annealing) is added on top of the structure before annealing at $750°C$ during $30min$ under secondary vacuum ($1.10^{-6}mbar$) to obtain the $L1_0$ phase of FePt. This process led to a coercive field $H_c = 1T$. The nanostructured active layer is deposited by RF sputtering under an homogeneous magnetic field (obtained by permanent magnets placed on the substrate holder). Alternating the sputtering of TbCo and FeCo composite targets led to 25 exchange-coupled $10nm$ bilayers ($250nm$ thick). FePt is finally polarized along HA. A typical result of this process is shown on fig.7. The vertical structure at the interface between FePt and Si is due to DRIE combined with masking effects.

Two sets of samples have been elaborated: 25 samples with centimeter dimensions on a 3" wafer with different geometric parameters ($L = 20, 50, 100, 200, 400\mu m$ and $L_{FePt}/L = 0.7, 0.6, 0.5, 0.4, 0.3$) and 5 samples fabricated on a thin ($150\mu m$) 2" silicon wafer to obtain centimeter-sized cantilevers for magnetoelastic characterizations.

V. RESULTS AND DISCUSSION

A. Magnetic characterizations

First measurements were made using a Vibrating Sample Magnetometer (VSM) equipment (ADE EV9 Series) with sub-μemu resolution. Fig.8 presents VSM measurements of the magnetization of a sample with the following characteristics: $L = 50\mu m$, $L_{FePt} = 25\mu m$, FePt thickness $e_{FePt} = 2\mu m$, Ta spacer thickness $e_{spacer} = 100nm$, active layer thickness $e = 250nm$. The contribution of FePt has been removed beforehand on the curve. As shown on fig.8, the global hysteresis curve $M(H_{ext})$ of the biased active layer along HA is composed of two shifted contributions (compared to the unbiased reference), each accounting for half of the magnetic stripes. Both shifts are almost symmetrical with a bias field of approximately $500Oe$. As, in some cases, slope changes are difficult to observe, we also used the derivatives of the hysteresis

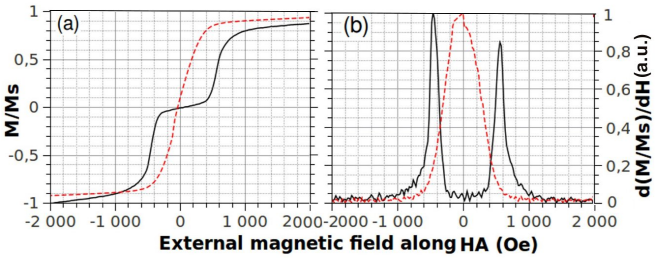

FIG. 8. Hysteresis curve (a) and derivative of the hysteresis curve (b) of the active layer (Solid: biased, dashed: unbiased). Sample Characteristics : $L = 50\mu m$, $L_{FePt} = 25\mu m$, FePt thickness $e_{FePt} = 2\mu m$, Ta spacer thickness $e_{spacer} = 100nm$, active layer thickness $e = 250nm$.[19]

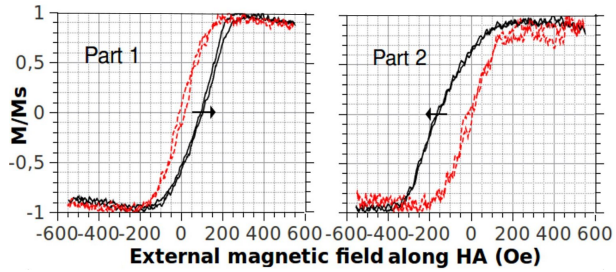

FIG. 9. MOKE measurements of a biased sample ($L = 100\mu m$, $L_{FePt} = 50\mu m$) (Solid: biased, dashed: unbiased).[19]

curves which are also presented on fig.8.

Longitudinal Magneto-Optic Kerr Effect (LMOKE) measurements have been carried out to investigate the magnetic microstructure on the surface of the nanostructured active layer and validate the interpretation of the VSM measurements. Due to size limitations of the experimental setup, measurements could not be carried out on every sample. Nevertheless, results obtained for $L = 100\mu m$, $L_{FePt} = 50\mu m$ confirmed our interpretations. The hysteresis curves for each part of the magnetic structure can be seen on fig.9. As expected, when FePt is magnetized, two adjacent stripes (namely part 1 and part 2) show opposite offsets along HA. Here, the offsets are respectively $100Oe$ and $200Oe$.

As stated above, the bias field must be equal to the anisotropy field to obtain the properties of SRT. Nevertheless, the biasing structure has been designed to provide a bias field superior to the anisotropy field. In such situation, the polarization can be taylored using minor magnetization cycles of FePt. Indeed, it is possible to reduce the bias field by reducing the remanent magnetization of the permanent-magnet elements. Fig.10 and Fig.11 illustrate the method: each half-loop lessens the shift of the magnetization cycle for both stripes. When FePt is fully demagnetized, the bias disappears.

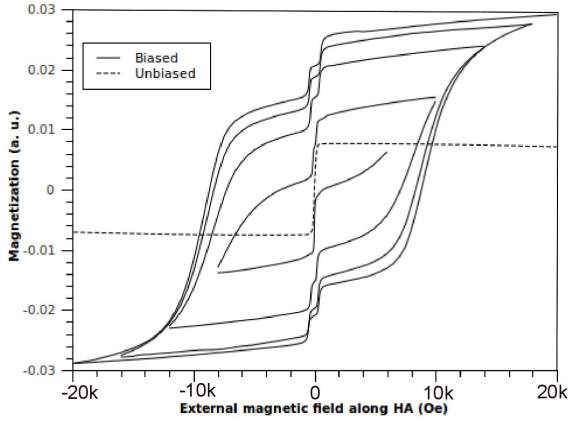

FIG. 10. Bias field adjustment by minor magnetization cycles.

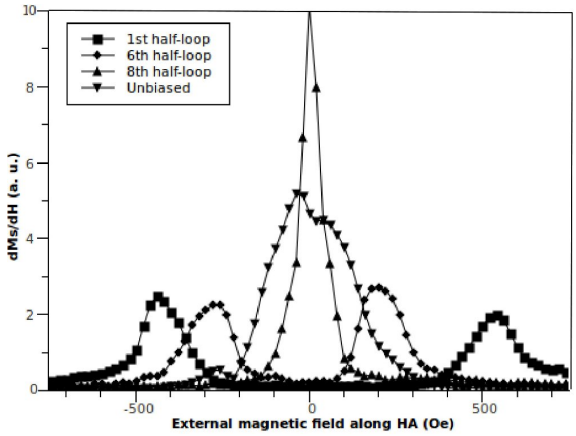

FIG. 11. Derivatives of the hysteresis curves for different minor magnetization cycles.

B. Magnetolelastic characterizations

Magnetoelastic characterizations have been carried out by a laser deflection technique on a centimeter sized silicon cantilever on top of which the biasing structure has been realized. The cantilever is placed inside the core of a driving coil producing a dynamic magnetic field along the EA of the active layer. The cantilever is then placed under an homogeneous static magnetic field created by an electromagnet along HA. The flexural or torsional vibration amplitude of the free tip is measured by the deflection of a laser beam on a 2D Position Sensing Diode (PSD). As predicted by theory[8], thanks to giant nonlinearity near the SRT, subharmonic magnetic excitation at $f_r/2$, with f_r a resonant frequency of the cantilever, results in an amplified mechanical vibration at f_r near the SRT point ($H_{Bias} \approx H_a$). Fig.12 shows the results for a $2cm \times 0.5cm \times 150\mu m$ cantilever for the second flexural mode at $f_r = 3124Hz$.

As expected, non-linear actuation of the system occurs for shifted values of the external magnetic field, compared to an unbiased sample, and even exists without any ex-

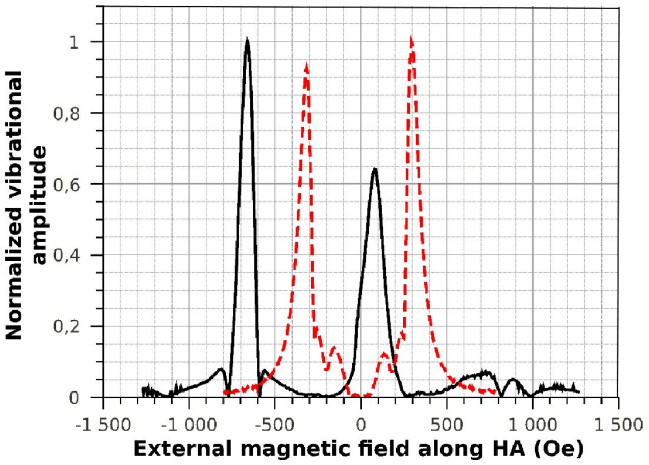

FIG. 12. Non-linear Magnetoelastic actuation measurement[19](Solid: biased, dashed: unbiased). Clamped cantilever: $2cm \times 0.5cm \times 150\mu m$. Excitation of the second flexural mode @ $f_r = 3124Hz$, excited with $f_{ex} = f_r/2 = 1562Hz$.

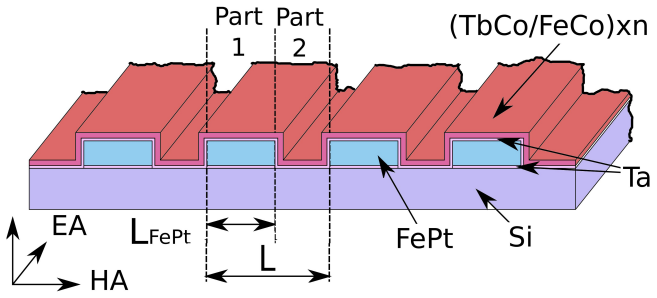

FIG. 13. Schematic view of the second biasing structure.

ternal field, as the bias field is close to the anisotropy field $H_a = 300Oe$.

C. Perspectives

The fabrication process presented above has proved efficient for our purposes. However, other structures can be considered. Following the same steps, we also investigated the potentialities of a simpler structure, presented on fig.13. The main asset of this structure is to reduce the technological complexity by suppressing the etching step.

First micromagnetic simulations have proved the viability of this approach. Fig.14 presents a simulation of such structure with the folowing parameters:$L = 50\mu m$, $L_{FePt} = 25\mu m$, FePt thickness $e_{FePt} = 2\mu m$, Ta spacer thickness $e_{spacer} = 100nm$, active layer thickness $e = 250nm$.

The technological realization is pending.

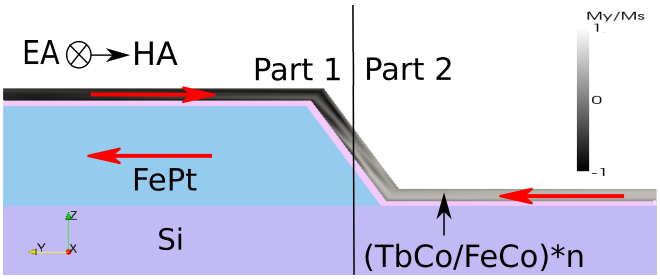

FIG. 14. Simulation of magnetization in the structure described in fig.13 (transverse view). Arrows indicate the main direction of magnetization.

VI. CONCLUSIONS

In this paper, we have proposed an integrated permanent magnet based microstructure for the polarization of nanostructured magnetic thin films exhibiting a Spin Reorientation Transition. Micromagnetic simulations proved to be efficient as a sizing and optimization tool for such structures. Several samples have been successfully elaborated thanks to a MEMS-compliant process. In the case of a giant magnetostrictive thin film, integrated (VSM) as well as local (LMOKE) magnetic characterizations confirmed the numerical studies. It was also found that the bias field could be taylored to fulfill the SRT requirements thanks to the minor magnetization cycles of FePt. Moreover, magnetoelastic measurements showed that, thanks to the integrated polarization, subharmonic actuation of a cantilever could be obtained, thus demonstrating the nonlinear behaviour expected in the vicinity of the SRT, without any external static field. Other structures are currently investigated to optimize the technological process. These results pave the way for the development and the integration of innovative and multifunctional Micro-Magneto-Mechanical-Systems (MMMS) and Micro-Magneto-Electro-Mechanical-Systems (MMEMS).

ACKNOWLEDGMENTS

This work is part of the French ANR PNANO-Project NAMAMIS. The authors would like to thank the Direction Générale de l'Armement(DGA-France) for the Ph.D. funding of Mr Y. Dusch, the French Ministry of foreign affairs (MAE) for the Ph.D. funding of Mr. Y. Ignatov, and Région Nord-Pas-de-Calais for the postdoctoral funding of Dr. V. Rudenko. In addition, the authors would like to thank Pr. D. Givord for fruitful discussions.

[1]H. Le Gall, J. BenYoussef, N. Tiercelin, P. Pernod, V. Preobrazhensky, and J. Ostorero, *Magnetics, IEEE Transactions on*, Magnetics, IEEE Transactions on DOI - 10.1109/20.908746 **36**, 3223 (2000), ISSN 0018-9464, 10.1109/20.908746.

[2]H. LeGall, J. BenYoussef, F. Socha, N. Tiercelin, V. Preobrazhensky, and P. Pernod (AIP, 2000) pp. 5783–5785, http://link.aip.org/link/?JAP/87/5783/1.

[3]H. Le Gall, J. BenYoussef, N. Tiercelin, V. Preobrazhsensky, P. Pernod, and J. Ostorero, *Magnetics, IEEE Transactions on*, Magnetics, IEEE Transactions on DOI - 10.1109/20.951279 **37**, 2699 (2001), ISSN 0018-9464, 10.1109/20.951279.

[4]H. LeGall, J. BenYoussef, N. Tiercelin, V. Preobrazhensky, and P. Pernod, Journal of the Magnetics Society of Japan **25**, 258 (2001), http://www.jstage.jst.go.jp/article/jmsjmag/25/3_2/25_258/_article.

[5]N. Tiercelin, J. BenYoussef, V. Preobrazhensky, P. Pernod, and H. L. Gall, Journal of Magnetism and Magnetic Materials **249**, 519 (Sep. 2002), ISSN 0304-8853, http://www.sciencedirect.com/science/article/B6TJJ-46DPFTB-9/2/4680a38dd98636f9e5c76ee8b97312b3.

[6]J. BenYoussef, N. Tiercelin, F. Petit, H. LeGall, V. Preobrazhensky, and P. Pernod, in *Magnetics Conference, 2002. INTERMAG Europe 2002. Digest of Technical Papers. 2002 IEEE International* (2002) p. AS5.

[7]N. Tiercelin, V. Preobrazhensky, P. Pernod, S. Masson, J. BenYoussef, and H. Le Gall, Mécanique & Industries **4**, 169 (May 2003), ISSN 1296-2139, http://www.sciencedirect.com/science/article/B6W74-48HXKVS-5/2/2d4f282c84211124b551febf1f49e968.

[8]N. Tiercelin, P. Pernod, V. Preobrazhensky, H. Le Gall, and J. BenYoussef, Ultrasonics **38**, 64 (Mar. 2000), ISSN 0041-624X, http://www.sciencedirect.com/science/article/B6TW2-3YWX3V2-F/2/cdb0aca7a69b445d48fe7925831073ba.

[9]N. Tiercelin, V. Preobrazhensky, P. Pernod, H. Le Gall, and J. BenYoussef, Journal of Magnetism and Magnetic Materials **210**, 302 (Feb. 2000), ISSN 0304-8853, http://www.sciencedirect.com/science/article/B6TJJ-3YF9XFW-1C/2/2aac90ed47a5d18c6c600595b5c5f161.

[10]N. Tiercelin, P. Pernod, V. Preobrazhensky, H. Le Gall, J. BenYoussef, P. Mounaix, and D. Lippens, Sensors and Actuators A: Physical **81**, 162 (Apr. 2000), ISSN 0924-4247, http://www.sciencedirect.com/science/article/B6THG-3YSXPYW-1C/2/6e2badc25502d525f02663cb66d16beb.

[11]A. Klimov, Y. Ignatov, N. Tiercelin, V. Preobrazhensky, P. Pernod, and S. Nikitov, J. Appl. Phys. **107**, 093916 (May 2010), http://link.aip.org/link/?JAP/107/093916/1.

[12]N. Tiercelin, V. Preobrazhensky, P. Pernod, and A. Ostaschenko, Appl. Phys. Lett. **92**, 062904 (Feb. 2008), http://link.aip.org/link/?APL/92/062904/1.

[13]N. Tiercelin, A. Talbi, V. Preobrazhensky, P. Pernod, V. Mortet, K. Haenen, and A. Soltani, Appl. Phys. Lett. **93**, 162902 (Oct. 2008), **Sélectionné pour le numéro du 3 novembre 2008 du Virtual Journal of Nanoscale Science & Technology**, http://link.aip.org/link/?APL/93/162902/1.

[14]N. Tiercelin, V. Preobrazhensky, V. Mortet, A. Talbi, A. Soltani, K. Haenen, and P. Pernod, *Selected papers from the Symposium F "Multiferroics and Magnetoelectrics Materials" of the E-MRS Conference*, Journal of Magnetism and Magnetic Materials **321**, 1803 (Jun. 2009), ISSN 0304-8853, http://www.sciencedirect.com/science/article/B6TJJ-4VM444C-1/2/8e0fdc5400c078d9428207dcfbb614e7.

[15]V. Neu, A. Anane, S. Wirth, P. Xiong, S. A. Shaheen, and F. J. Cadieu, "Design optimization for a smco-biased colossal magnetoresistive thin film device," (2000), 10.1063/1.373344.

[16]M. Kitada, Y. Kamo, H. Tanabe, H. Tsuchiya, and K. Momata, J. Appl. Phys. **58**, 1667 (Aug. 1985), http://link.aip.org/link/?JAP/58/1667/1.

[17]L. Landau and E. Lifshitz, *Course of Theoretical Physics; statistical physics* (Ellipses, 1994).

[18]J. Peuzin, A. Garnier, K. Mackay, V. Mandrillon, and S. Sarkozi, in *Proceedings of the French Journée microsystèmes du CNRS* (1999) p. 55, paris.

[19]Y. Dusch, N. Tiercelin, A. Klimov, V. Rudenko, Y. Ignatov, S. Hage-Ali, P. Pernod, and V. Preobrazhensky, Journal of Applied Physics.(2011), submitted.

[20]D. Meeker, "Finite element method magnetics, version 4.0.1, (03dec2006 build), http://www.femm.info," Tech. Rep.

[21]W. Scholz, J. Fidler, T. Schrefl, D. Suess, R. Dittrich, H. Forster, and V. Tsiantos, *Proceedings of the Symposium on Software Development for Process and Materials Design*, Computational Materials Science **28**, 366 (Oct. 2003), ISSN 0927-0256, http://www.sciencedirect.com/science/article/B6TWM-49HDWCS-4/2/dfb3dd3c80f60d26dbedd2d79bbddded.

[22]A. Walther, C. Marcoux, B. Desloges, R. Grechishkin, D. Givord, and N. Dempsey, *Current Perspectives: Perpendicular Recording*, Journal of Magnetism and Magnetic Materials **321**, 590 (Mar. 2009), ISSN 0304-8853, http://www.sciencedirect.com/science/article/B6TJJ-4TKX0K7-3/2/60198ff5101b78e55cea885a865e54e5.